

# Formation of Microgel Beads by Electric Dispersion of Polymer Solutions

**D. Poncelet**

ENSAIA, BP 172, 54505 Vandoeuvre, France

**R. J. Neufeld**

Queen's University, Kingston, Canada K7L 3N6

**M. F. A. Goosen**

Sultan Qaboos University, 123 Muscat, Sultanate of Oman

**B. Burgarski**

University of Belgrade, 11000 Beograd, Yugoslavia

**V. Babak**

INEOS RAS, Vasilova str. 28, Moscow 117813, Russia

*Microcapsules are produced by a dropwise addition of one solution into a solidifying bath. By applying an electrostatic potential between the droplet formation device and the collecting solution, it is possible to obtain smaller droplets which are desirable for many applications. Droplet formation may be divided into two phases. Under a certain critical value of the electric potential  $U_c$ , liquid exits the nozzle as droplets. The surface tension decreases with increasing electric potential resulting in a reduction of droplet diameter to approximately 200  $\mu\text{m}$ . At higher electric potential, liquid exits the nozzle as a jet which subsequently breaks into droplets, which are smaller than 200  $\mu\text{m}$ . In this case, droplet size is mainly determined by the jet instability (theory of Rayleigh).*

## Introduction

Microencapsulation generally involves two steps: drop formation (discrete droplet formation or emulsification), followed by droplet solidification (gelation, membrane formation, or other means). The most widespread laboratory method is by extrusion of polymer droplets containing the immobilizant through a needle, then into a gel forming solution, solidifying the falling droplets in microbeads or capsules. The main drawback of the droplet extrusion method is the large size (greater than 1 mm) of the resultant beads and the low rate of the bead formation (Poncelet et al., 1994).

A significant decrease in the droplet diameter may be realized by applying an electric potential between the polymer solution and the collecting solution during dropwise extrusion from the needle (Figure 1a), as described by several authors (Kershavarz et al., 1992; Bugarski et al., 1994; Poncelet,

1994). A characteristic feature of this technique is a gradual decrease of droplet diameter  $d$  with increasing applied electric potential  $U$  up to the critical electric potential  $U_c$ . Further increase in electric potential  $U$  results in the formation of unstable liquid jets, which fragment into droplets with diameters of 100  $\mu\text{m}$  and below (Figure 1b). The droplet diameter  $d$  depends on several physico-chemical and technological parameters such as internal diameter of the needle capillary  $d_c$ , liquid flow rate  $j_v$ , polarity of applied electric potential, geometry of droplet apparatus, and so on.

In spite of the importance of this technique for scale-up in the encapsulation industry, the mechanism of the electrostatic generation of droplets from liquid jets is not completely understood. This makes the design of industrial equipment for the production of immobilized biocatalysts and the control of hydrogel bead size difficult. The objective of this article is to evaluate the observed effects of physico-chemical parameters on the dispersion process under applied electric potential of high voltage.

Correspondence concerning this article should be addressed to D. Poncelet at his new address: ENITIAA, 44 322 Nantes Cedex 3, France.

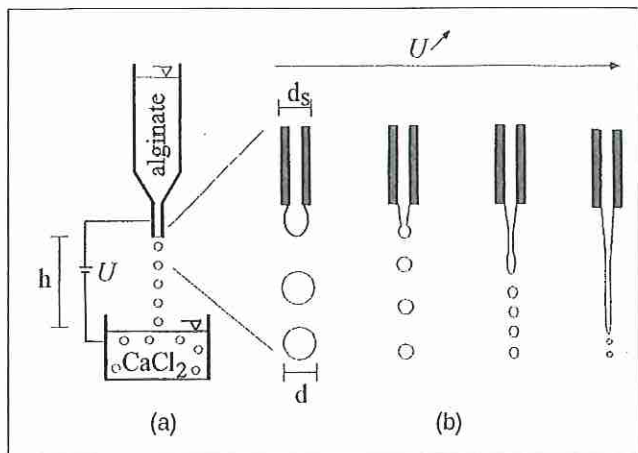


Figure 1. Electrostatic droplet generator (a) Droplet formation process vs. electric potential  $U$  (b).

## Materials and Methods

### Chemicals

Sodium alginate of low (S170), medium (S550), and high viscosity (S1160) was obtained from Sanofi (Paris, France). Calcium chloride was purchased from BDH (Toronto, Canada).

**Droplet Formation Using Electrostatic Droplet Generator (Figure 1).** Alginate beads have been selected as a model. Nearly 90% of the cell encapsulation literature refers to this system. Moreover, they are simple to form and results of the size dispersion may extrapolate to other types of gel beads and microcapsules.

A 1.8% alginate solution was forced through a needle tip (16s, 22s, 22s, and 26 Gauges; 90° blunt needles, Chromatographic Specialties Inc., Brockville, Canada) with the help of a syringe pump (36 mL/h, Razel Scientific Instruments, Stamford, CT). An electric potential was applied between the needle and the collecting solution (1.5%  $\text{CaCl}_2$ ) using an electrostatic power supply (Model 30R, Bertan Associates, Inc., New York) with a maximum current of 0.4 mA and variable voltage of 0 to 30 kV. The needle tip was mounted 2.5 cm, 3.5 cm, and 4.8 cm above the collecting solution.

**Analysis of the Droplet Formation Using Image Analysis.** The image analysis system consisted of a video camera (Panasonic Digital 5100), video Adapter (Sony Trinitron PVM1342Q), VHS recorder (Panasonic NV8950), and the results were analyzed with java version 1.3 software for image analysis (Jandel scientific, CA). For close-up studies of droplet formation, the video was connected to a microscope lens (Olympus SZH, Japan). Droplet images were frozen under a strobe light (Stobotac, GRC, MA) at defined frequencies between 50 and 400 hz.

**Determination of Microbead Size Distribution.** Volumetric (volume of microspheres in each diameter class) and volumetric cumulative bead size distributions were determined by laser light scattering using a 2602-LC particle analyzer (Malvern Instruments) according to a log-normal distribution model. The mean diameter  $d_{50}$  was evaluated at 50% of the cumulative volume fraction. Resolution of the size has been evaluated to less than 10% by replications of the measurement.

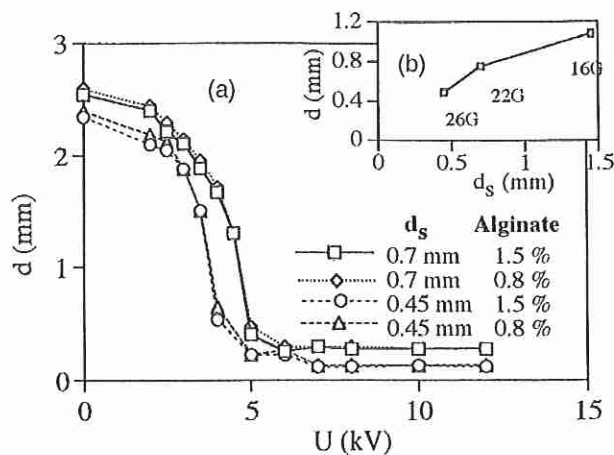


Figure 2. Droplet diameter  $d$  in function of electric potential  $U$ .

(a) Effect of needle diameter  $d_s$  and alginate concentration; (b) effect of needle diameter  $d_s$ .

## Experimental Studies

Figures 1b and 2a illustrate the evolution of the pendant droplet formation and droplet size as a function of the applied electric potential  $U$ . A sharp decrease of the droplet diameter  $d$  from approximate 1 mm (Figure 2a) to less than 0.1 mm was observed with increasing electric potential  $U$ . At a critical value  $U_{cr}$ , unstable liquid jets of the polymer solution form and disintegrate into multiple microscopic charged droplets (Figure 2a).

Different parameters were evaluated to control the size of the droplets. Electrode spacing was not found to be significant over the range investigated (Figure 3a). However, Nabab and Mason (1958) observed that at lower electrode spacing (0.1 to 1.2 cm), the jet may split into fine treads which break into very fine monodispersed droplets (2  $\mu\text{m}$ ).

Alginate concentration, and, consequently, the viscosity, seem to have very little impact on bead diameter (Figure 2a).

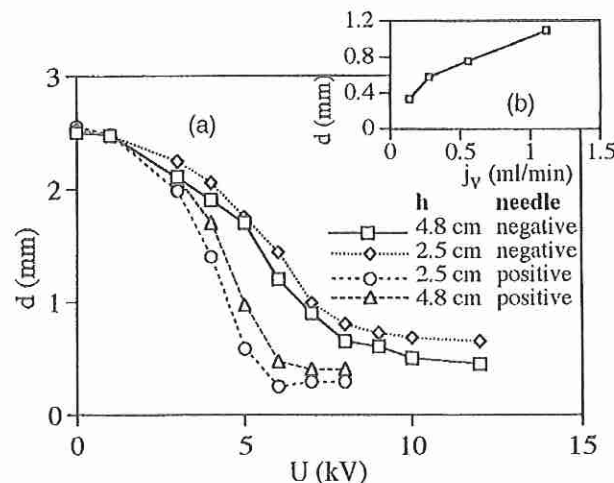


Figure 3. Droplet diameter vs. (a) electrode spacing, needle polarity; (b) impact of the flow rate.

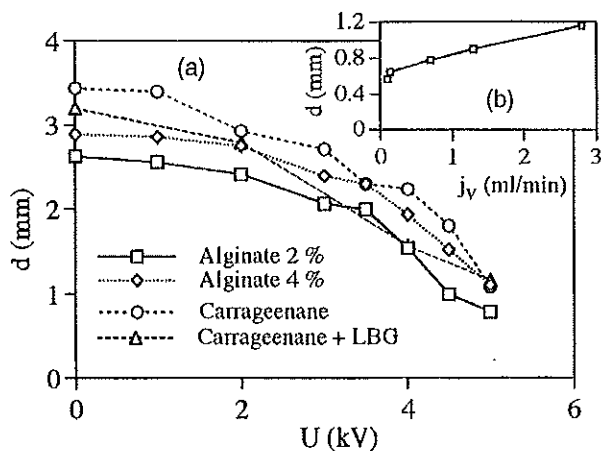


Figure 4. Effect of the electric potential  $U$  on the droplet diameter  $d$ .

(a) Impact of the extruded solution nature; (b) influence of the flow rate (data extracted from Kershavarz et al., 1992).

Moreover, different polymer solutions (alginate of different grades, K-carrageenane, K-carrageenane + locust bean gum) only has a weak effect on the beads size (Figure 4a). The difference between curves may be attributed to the level of shrinking during gelation of the different type of beads.

Except for the electric potential itself, three other parameters have a strong effect on bead diameter. Increasing the flow rate  $J_v$  of polymer solution results in an increase in the bead diameter, as shown in Figure 3b and 4b. Reducing the needle diameter results in smaller droplets (Figures 2a and 2b) and, finally, the polarity of the dropping device affects the size of the beads. A positively charged needle results in smaller drops, and the critical electric potential  $U_{cr}$  required to attain jet formation, decreases as shown in Figure 3a.

It should be noted as well that an earlier study demonstrated that the geometry of the dropping device affects both the size of the drop and the effect that the parameters described above have on the droplet size (Bugarski et al., 1994; Poncelet et al., 1994).

## Discussion and Process Modeling

The application of electrical potential in droplet extrusion results in smaller droplets than under simple gravity. However, the behavior of the system appears quite complex. In previous studies (Kershavarz, et al., 1992; Poncelet et al., 1994; Burgarski et al., 1994), different models have been described. However, they do not adequately explain the different experimental observations, although the role of the controlling parameters is now better understood. This section summarizes the understanding of the droplet formation.

### Formation of hydrogel beads by droplet extrusion

A pendant droplet which is formed by extruding a liquid from the tip of a capillary tube continuously grows until it achieves a critical mass  $m$ . The droplet then detaches and falls into a receiving solution. In the absence of an electric field  $m$  may be defined by the equilibrium between the gravity force ( $mg$ ) and the surface tension force ( $\pi d_s \gamma$ ) at the

breakage point

$$mg = \frac{\pi d_o^3}{6} \rho g = \pi d_s \gamma \quad (1a)$$

or

$$d_o = \sqrt[3]{\frac{6 d_s \gamma_o}{\rho g}} \quad (1b)$$

where  $g$  is the gravitational constant,  $\rho$  is the density of the polymer solution, and  $d$  is the diameter of the falling drop (index  $o$  refers to the system in absence of any other force but gravity),  $d_s$  is the diameter of the pendant droplet neck, and  $\gamma$  is the surface tension acting at the moment of droplet detachment.

The surface tension  $\gamma$  of aqueous polymer solutions is  $40 \text{ mJ} \cdot \text{m}^{-2}$ , the solution density is  $1 \text{ kg} \cdot \text{l}^{-1}$ , and the diameter of the pendant droplet neck  $d_s$  is approximately equal to the external diameter of the capillary needle  $d_e$  (0.5 to 1 mm). The diameter  $d_o$  of droplets cannot then be reduced to less than 1 mm in simple droplet extrusion in the absence of other forces with the exception of gravity.

### Diameter of falling droplet subject to an electric force

The condition for the mechanical equilibrium of a pendant droplet in an electric field may be written in the form

$$\frac{\pi d^3}{6} \rho g + F_e = \pi d_s \gamma \quad (2a)$$

or

$$\delta = \frac{d}{d_o} = \sqrt[3]{1 - \frac{6F_e}{d_s \gamma}} \quad (2b)$$

The electric force  $F_e$  depends on the geometry of the experimental setup. For example, in the case of a single needle situated in the proximity of a plane electrode as is the case with a collecting solution (Figure 1), its value may be expressed as

$$F_e = \pi \epsilon_o \left( \frac{d}{2h} U \right)^2 \quad (3)$$

where  $\epsilon_o$  is air electric permittivity,  $h$  is the distance between the droplet and the plane electrode, and  $U$  is the applied electric potential. This equation is valid for a droplet in the proximity of a plane electrode (collecting beaker) with a diameter that is larger than 3 times the distance between the liquid and the drop  $h$ .

Equation 3b provides a poor fit to the experimental data. First, while increasing electric potential, the experimental droplet diameter  $d$  decreases faster than expected as seen in Figure 5. Experimentally, the size of the drop is independent of the distance between the droplet and collecting solution  $h$ .

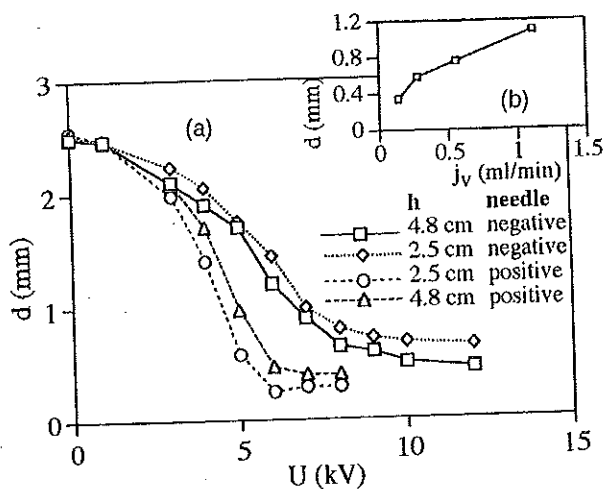


Figure 5. Modeling of the reduced droplet diameter  $d$  vs electric potential  $U$ .

Equation 3b also doesn't explain the effect of the flow rate or the droplet polarity, and jet formation at higher electric potential. In fact, the electric force  $F_e$  would have a significant effect only if the distance  $h$  is very low.

It is then necessary to search for another cause for the droplet-size reduction then subject to a electric potential.

#### Electrocapillary effects in the droplet extrusion process

Surface tension  $\gamma$  or the attraction between liquid molecules at the surface of the drop is the main force maintaining the pendant droplet on the needle. By applying an electric potential, the migration of charged molecules to the surface of the droplet is promoted. These molecules will repulse each other, causing the surface tension to decrease. According to Lippman's theory of electrocapillarity (Hunter, 1989), the equilibrium surface tension  $\gamma$  of a charged liquid surface decreases with increasing electrical potential  $U$  as

$$d\gamma = -\sigma dU \quad (4)$$

where  $\sigma$  is the electric surface charge. Assuming the pending droplet as a sphere, submitted to the electric potential  $U$  the mean surface density of the electric charge  $\sigma$  may be expressed as

$$\sigma \approx \frac{q_o}{\pi d^2} = 2\epsilon_o \frac{U}{d_c} \quad (5)$$

Combining Eq. 4 and 5 and integrating over the electric potential  $U$  gives an expression of the surface tension  $\gamma$  in function of electric potential  $U$

$$\gamma = \gamma_o \left(1 - \frac{\epsilon_o U^2}{d_c \gamma_o}\right) = \gamma_o \left(1 - \frac{U^2}{U_c^2}\right) \quad (6)$$

where  $\gamma_o$  is the surface tension of a liquid at  $U = 0$ , and  $U_c$  is the critical electrostatic potential as defined below. Neglecting electric force  $F_e$ , the equilibrium balance between the

force acting on the pendant droplet may be obtained by combining Eqs. 1 and 7

$$mg = \frac{\pi d^3}{6} \rho g = \pi d_s \gamma_o \left(1 - \frac{U^2}{U_c^2}\right) \quad (7a)$$

or

$$\delta = \frac{d}{d_o} = \sqrt[3]{\left(1 - \frac{U^2}{U_c^2}\right)} \quad (7b)$$

Equation 16 remains valid until the electric potential decreases to the critical value  $U_c$

$$U_c \approx \sqrt{\frac{d_c \gamma_o}{\epsilon_o}} \quad (8)$$

Near this value, the surface tension becomes negligible and the liquid droplet becomes unstable (Figure 1). Depending on the conditions, the liquid will then exit the needle as a jet, and the size of the droplets become quasi independent of the applied electric potential.

Equation 7b allows to simulate more accurately the experimental data (Figure 5). The size of the drop is no longer a function of the drop-to-collecting solution distance  $h$  and the theoretical curves better fit the experimental data, as shown in Figure 5. Jet formation is attributed to elimination of surface tension. However, some effects are still not taken in consideration, that is the effects of polarity and liquid flow rate.

#### Nonequilibrium conditions

The main simplifying assumption was to describe assimilating the liquid droplet as an ideal electric conducting sphere. The electric charge that accumulated on the droplet is determined by the adsorption of counterions, ionic surfactants, and ionized functional groups of macromolecules drawn to the droplet surface. The adsorption of the electric charge may be limited by the sterical hindrance of these bulky electric carriers, and their diffusion rate to the droplet surface. The dependence of the droplet charge  $q$  on the electric potential  $U$  may differ from that derived for the idealized conductors. Equation 14 may be rewritten as follows

$$\gamma = \gamma_o \left(1 - k' \frac{U^2}{U_c^2}\right) \quad (9)$$

where  $k'$  describes the nonequilibrium state.  $k'$  may also take into account the nonsphericity of the droplet, the influence of the needle on the charge distribution, and so on.

A first approach to investigate the nonequilibrium state is to compare the time to form one drop  $\tau_v$  with the characteristic time of surface active component adsorption at the droplet surface  $\tau_a$ . Droplet formation time  $\tau_v$  is given as

$$\tau_v = \frac{\pi d^3}{6} j_v \quad (10)$$

where  $j_v$  is the liquid flow. In hydrogel bead production, the flow is generally in the range of 0.1 to 3 mL/min. The droplet formation time then ranges from 3 to 90 ms. The characteristic time of adsorption  $\tau_a$  may be approached by assuming that the molecules diffuse (Brownian motion) from the center of the bead to the droplet surface (Einstein, 1906)

$$\tau_a = \frac{2d^2}{D} \quad (11)$$

where  $D$  is the diffusion coefficient of the surface active molecule.

For low molecular weight ions, in the absence of an electric field, the diffusion coefficient  $D$  is around  $10^{-8} \text{ m}^2 \cdot \text{s}^{-1}$ . The characteristic time  $\tau_a$  is then larger than 10 s or two orders of magnitude  $\tau_v$ . A very limited amount of surface active material will have time to reach the surface during the droplet formation. The surface tension  $\gamma$  will then mainly be equal to the pure water  $\gamma_0$  independently of the active surface component addition to the system.

When subject to an electric field, the diffusion coefficient of ionic molecules is increased proportional to  $(FU/RT)^{1/2}$ , where  $F$  is the Faraday constant. For electric potential ranging from 1 to 10 kV, the absorption characteristic time  $\tau_a$  is expected to be 100 to 1,000 times lower than in absence of electric potential. For low molecular weight molecules (counterions or small ionic surfactant) under electric potential, the ratio  $\tau_a/\tau_v$  is consequently near 1. The surface tension  $\gamma$  will then be defined by Eq. 18, and beads size function of the electric potential  $U$ .

For macromolecules, the diffusion coefficient  $D$  may be considered to be at least 100 times smaller. Even when applying an electric potential  $U$ , the ratio  $\tau_a/\tau_v$  remain large. While the surface active component is a polymer, the surface tension would remain near the value of the water. Bead size is only slightly dependent of the electric potential  $U$  and remains large.

#### Effect of the droplet polarity on the droplet size

According to the above developments, the effect of the system polarity on the process, and particularly on the droplet size  $d$ , may be predicted. Using sodium alginate solution droplet formation as an example, when a positive electric potential is applied to the needle,  $\text{Na}^+$  cations migrate quickly and are absorbed at the droplet surface. The surface tension decreases leading to smaller beads.

However, in the case of a negatively charged needle, the negatively charged alginate polyelectrolyte must migrate from the solution to the surface. Using previous considerations, one would expect that the relaxation time  $\tau_a$  will be much greater than for  $\text{Na}^+$  ions because of the lower diffusional mobility of macromolecules with regard to the counterions. For given electric potential and flow rate, the surface density of the electric charge  $\sigma$  will be lower for the negatively charged needle, and, consequently, the surface tension will be greater. This will result in a larger droplet size and critical potential for the negatively charged needle compared to the positive one (in case of alginate beads).

#### Effect of the flow rate on the droplet size

While the ratio of the characteristic times  $\tau_a/\tau_v$  is very large ( $> 100$ ) or very low ( $< 0.01$ ), the surface tension is respectively equal to its value for pure water and near to zero. However, in an intermediate range, changing the flow rate will influence the quantity of the active surface molecule moving to the droplet surface and then the surface tension. Consequently, the droplet diameter decreases with decreasing flow rate.

#### Effect of viscosity on droplet size

The viscosity of the polymer solution and the selection of hydrogel composition on the droplet size was observed to have an insignificant effect on the droplet size. A droplet under formation may be viewed as a bag being filled by the liquid flow. The slower the process of closing the bag, the larger will be the resulting droplet. The viscosity may be compared with the pressure acting on the droplet surface or the capillary pressure  $P_c$  as  $\gamma/d$ . The characteristics time for the viscous liquid droplet is then given by

$$\tau_\eta = \frac{\eta}{P_c} \quad (12)$$

which is lower than 0.1 ms for polymer solutions of viscosities in the range from  $10^{-3}$  to  $10^{-2} \text{ Pa} \cdot \text{s}^{-1}$  compared to the characteristic time of droplet formation, ranging from 3 to 90 ms. So, the droplet formation process, and consequently the diameter of droplets, is not affected by the variation of the viscosity of polymer solutions in the range from  $10^{-3}$  to  $10^{-2} \text{ Pa} \cdot \text{s}^{-1}$ .

#### Critical electric potential and jet formation

As stated above, when the electric potential approaches the critical electric potential, the liquid exits the nozzle as a jet. With a single needle, the critical electric potential did not exceed 5 kV and manifested a slight dependence on the needle diameters. The value of critical electric potential did not depend on the distance  $h$  between the electrodes in the range between 2.5 and 4.8 cm and formed the decreasing series (kV): 5.0; 4.7 and 4.2 for the corresponding series of needle diameters (mm): 0.71 mm (22 G), 0.63 (23G), and 0.50 (26G). This dependence correlates well with the law  $U_{cr} \approx d^{1/2}$  predicted by Eq. 8.

The jet breaks into small droplets due to instability (Rayleigh, 1878). The droplet diameter is mainly determined by the jet diameter and equal to approximately two times the jet diameter. More experiments are required to correlate jet and droplet diameters with the physico-chemical properties and electrostatic potential.

#### Conclusions

Applying electrostatic potential appears to be one interesting solution to obtain small droplets for the formation of small monodispersed microspheres and microcapsules. The size dispersion remains low (standard deviation 15%) (Burgarski,

et al., 1994) compared to spray methods (SD 35%). Further experiments are required to more fully understand and control droplet formation. By combining jet formation under electrostatic potential with jet breakage by vibration, it is expected that small microcapsules with a narrow size distribution may be prepared. For laboratory applications, the present design is suitable, but it is necessary to design a system with higher flow rates for pilot- and industrial plant-scale operations.

#### Literature Cited

- Bugarski, B., B. Amsdem, R. J. Neufeld, D. Poncelet, and M. F. A. Goosen, "Effect of Electrode Geometry and Charge on the Production of Polymer Microbeads by Electrostatics," *Canadian J. of Chem. Eng.*, **72**, 517 (1994).
- Bugarski, B., Q. Li, M. F. A. Goosen, D. Poncelet, R. J. Neufeld, and G. Vunkak, "Electrostatic Droplet Generation: Mechanism of Polymer Droplet Formation," *AIChE J.*, **40**, 1026 (1994).
- Einstein, A., "Zur Theorie der Brownschen Bewegung," *Annalen der Physik*, **19**, 371 (1906).
- Hunter, R. J., *Foundations of Colloid Science*, Vol. 1, Oxford University Press, New York (1989).
- Keshavarz, T., G. Ramsdem, P. Phillips, P. Musenden, and C. Bucke, "Application of Electric Field for Production of Immobilized Biocatalysts," *Biotechnol. Techniques*, **6**, 445 (1992).
- Nabab, N. A., and S. G. Mason, "The Preparation of Uniform Emulsion by Electrical Dispersion," *J. Colloid Sci.*, **13**, 174 (1957).
- Poncelet, D., B. Poncelet De Smet, C. Beaulieu, and R. J. Neufeld, "Scale-up of Gel Bead and Microcapsule Production in Cell Immobilization," *Fundamentals of Animal Cell Encapsulation and Immobilization*, M. F. A. Goosen, ed., CRC Press, Boca Raton, FL (1992).
- Poncelet, D., B. Bugarski, B. G. Amsdem, J. Zhu, R. J. Neufeld, and M. F. A. Goosen, "A Parallel Plate Electrostatic Droplet Generator: Parameters Affecting Microbead Size," *Appl. Microbiol. and Biotechnol.*, **42**, 251 (1994).
- Rayleigh, J. W. S., "On the Instability of Jet," *Proc. of London Mathematics Soc.*, **10**, 4 (1878).

Manuscript received Sept. 22, 1998, and revision received Apr. 18, 1999.